Kaur, Parminder; Khan, Moonis Ali; Li, Yongdan; Al-Othman, Ahmed A.S.; Alothman, Zeid Abdullah; Sillanpää, Mika; Kuokkanen, Ville; Imteaz, Monzur A.; Al-Farraj, Saleh

Investigating the effectiveness of bifacial mixed metal MOF electrodes for the photoelectro-catalytic treatment of municipal wastewater

Published in:
Journal of Cleaner Production

DOI:
10.1016/j.jclepro.2023.136165

Published: 15/03/2023

Document Version
Publisher's PDF, also known as Version of record

Journal of Cleaner Production 392 (2023) 136165

Contents lists available at ScienceDirect

Journal of Cleaner Production

journal homepage: www.elsevier.com/locate/jclepro

Investigating the effectiveness of bifacial mixed metal MOF electrodes for the photoelectro-catalytic treatment of municipal wastewater

Parminder Kaur [a,*], Moonis Ali Khan [b], Yongdan Li [a], Ahmed A.S. Al-Othman [c], Zeid Abdullah Alothman [b], Mika Sillanpää [d,e,**], Ville Kuokkanen [f], Monzur A. Imteaz [g], Saleh Al-Farraj [h]

[a] Department of Chemical and Metallurgical Engineering, Aalto University, Espoo, 00076, Finland
[b] Chemistry Department, College of Science, King Saud University, Riyadh, 11451, Saudi Arabia
[c] Department of Agricultural Engineering, College of Food Sciences and Agriculture, King Saud University, P.O. Box 2460, Riyadh, 11451, Saudi Arabia
[d] Environmental Engineering and Management Research Group, Ton Duc Thang University, Ho Chi Minh City, Viet Nam
[e] Faculty of Environment and Labour Safety, Ton Duc Thang University, Ho Chi Minh City, Viet Nam
[f] Kierto Ympäristöpalvelut Oy, Levysepänkaari 7-9, 04440, Järvenpää, Finland
[g] Department of Civil and Construction Engineering, Swinburne University of Technology, Melbourne, Australia
[h] Department of Zoology, College of Science, King Saud University, Riyadh, Saudi Arabia

ARTICLE INFO

Handling Editor: Prof. Salonitis Konstantinos

Keywords:
Photoelectro-catalytic process
Metal-organic framework
Municipal wastewater
Chemical oxidation demand
Visible light
Disinfection

ABSTRACT

The effectiveness of bifacial mixed metal-metal organic framework (MOF) anodes for municipal wastewater's photoelectro-catalytic (PEC) treatment has been rarely explored. Herein, pollutants removal efficiency from the municipal wastewater and the effect of operational parameters is verified under a visible range of light in a PEC system using TiO_2–Bi(mixed metal)-MOF and TiO_2–Sb(mixed metal)-MOF anodes, respectively. The comparable efficiency of pollutant removal from municipal wastewater in the PEC system with TiO_2–Bi(mixed metal)-MOF anodes is high. At optimum operation parameters, TiO_2–Bi(mixed metal)-MOF anodes in the PEC system play a positive role in the removal of micropollutants and the disinfection of municipal wastewater. This study reveals that PEC treatment of municipal wastewater contributes (35% of relative luminescence inhibition) to toxic biproducts.

1. Introduction

In recent decades, different types of environmentally malign wastewater are generated in huge volumes (reaching billions of liters per day) on a global scale (Linares-Hernández et al., 2009). Most of them contain higher levels of chemical oxygen demand (COD), biochemical oxygen demand (BOD), and micropollutants. Among them, municipal wastewaters are a major source of macro and micropollutants (pharmaceuticals, hormones, and personal care products), and require effective measurements for regulation and control (Vineyard et al., 2021). Recently, the concentrations of pharmaceuticals found in the aquatic environment have significantly increased. The existence of such compounds in the wastewater contributes to high COD value, micropollutants, and toxicity (Lecomte et al., 2017; Panter et al., 2000). Municipal wastewater has been treated using various conventional methods. Nowadays, the conventional chemical coagulation method is mostly used in water and wastewater treatment plants. The other commonly used methods for water and wastewater treatment are physical methods (such as filtration, screening, and sedimentation/-flotation), physicochemical methods (such as coagulation, adsorption, and ion exchange), various types of biological processes (such as activated sludge processes, trickling filtration, and various types of ponds and lagoons), membrane processes (such as reverse osmosis), disinfection methods (such as chlorination, ozonation, or ultraviolet proc), and disinfection methods, etc. (AWWA, 1999; Eckenfelder et al., 2009). However, municipal wastewater comprises several micro and macro pollutants that are difficult to remove using conventional treatment methods (Top et al., 2020). Hence, electrochemical methods such as electrocoagulation (EC), electroflotation (EF), electro-oxidation (EO), and electrodialysis (ED) have recently gained more attention (Chen et al., 2000; Särkkä et al., 2015; Kaur, 2019; Kaur et al., 2020;

* Corresponding author.
** Corresponding author. Environmental Engineering and Management Research Group, Ton Duc Thang University, Ho Chi Minh City, Viet Nam.
E-mail addresses: parminder.kaur@aalto.fi, kaur.parminder663@gmail.com (P. Kaur), mika.sillanpaa@tdtu.edu.vn (M. Sillanpää).

https://doi.org/10.1016/j.jclepro.2023.136165
Received 17 February 2022; Received in revised form 30 December 2022; Accepted 22 January 2023
Available online 30 January 2023

Abbreviations

MOF	Metal-organic framework
PEC	Photoelectro-catalytic
COD	Chemical oxygen demand
BOD	Biochemical oxygen demand
EO	Electro-oxidation
BET	Brunauer–Emmett–Teller
SSA	Specific surface area
EEC	Electrocatalytic Energy Consumption
CE	Current efficiency

Kuokkanen et al., 2021; Vineyard et al., 2021). The feasibility of the aforementioned technologies depends on the application in question, and each of them has its advantages and disadvantages. Consequently, there is an urgent need for the development of more effective water and wastewater treatment methods.

Photo-electrocatalysis (PEC), an advanced chemical oxidation process for the degradation of organic pollutants, is light-driven and it combines the advantages of both photocatalysis and electrocatalysis (Cheng et al., 2019; Collivignarelli et al., 2021). It is an attractive alternative method in wastewater treatment due to its high effectiveness, shorter treatment time, low cost, and simplicity (Kiama and Ponchio, 2021). Furthermore, no chemicals are required for this method, which makes PEC a green technology. The synergy of photocatalytic and electrochemical processes is visible both from the point of view of the photocatalytic process, which increases its efficiency as the bias potential reduces recombination of the photogenerated charges, but also from the electrochemical perspective, as depolarizing of the cell is allowed by the photogenerated potential on the semiconductor, therefore minimizing the costs of the overall process (Cheng et al., 2019; Palmas et al., 2021). To achieve the required bias potential, a good photo and electroactive materials are a necessity.

TiO_2 has been broadly used as a model photocatalyst in photocatalysis system as it is a cost-effective, non-toxic, and stable semiconductor (Cheng et al., 2019; Xu et al., 2009). However, the application of TiO_2 in water treatment is suppressed due to its wide bandgap (3.2 eV) and rapid photoinduced carrier recombination (Cheng et al., 2019; Palmas et al., 2021). To tackle this problem, various TiO_2 modifications have been investigated (Zhang et al., 2018; Ling et al., 2018). Simultaneously, another important research target in the literature has been the search for the best novel visible light active photocatalysts (Cheng et al., 2019). The practical approach to rectify the issue is to widen the bandgap of TiO_2 by adding a metal impurity as an intrinsic impurity into the semiconductor's crystal lattice in the form of a framework. This generates an intermediate energy level between the conduction and valence bands, providing a location for electron excitation with minimum energy consumption and photon requirements, eventually preventing rapid electron-hole pair recombination by boosting interfacial charge transfer (Lopez et al., 2020).

In the present study, a set of mixed metals-metal-organic framework layered TiO_2 electrodes were chosen to drive the PEC under visible light (500 nm) (Feng et al., 2019; Zhang et al., 2018; Su et al., 2008). The Construction of a heterostructure between metals and semiconductors to improve photocarrier separation and inhibit recombination is a particularly effective method among these attempts. Hybridization of metals in the form of a framework provides better photo-electrocatalytic efficiency than pure metals. Antimony and bismuth have typical properties to construct heterojunctions with metals and improve their photo and electric catalytic activity (Shi et al., 2019).

Moreover, Metal-organic frameworks (MOFs) are currently under vigorous research, and MOFs along with their derivatives have provided a vast amount of new electrode materials. MOFs and MOF-derivatives offer a lot of structural flexibility (such as metal nodes, ligands, and pore structure) and metal ions with redox activities therefore they have a great potential for usage in various energy devices. High energy capacities, greater specific surface areas, low density, and huge internal pore volumes distinguish these materials. As a result, in addition to their regular uses in chemical sensing and renewable energy, these materials have gained huge attention in supercapacitor applications (Tan et al., 2021; Du et al., 2018; Dubal et al., 2019). Although mixed MOFs have also been studied for high-performance hybrid supercapacitors with promising results (Han et al., 2021), they are yet to be used as electrodes for the PEC process.

Since, the presence of synergistic effects or more catalytic active sites, mixed-metal MOFs frequently outperform parent MOFs. Mixed-metal MOFs can be used as an important developing platform for the fabrication of novel photoactive and conductive materials.

This work aims to synthesize working mixed metal (TiO_2–Bi-MOF and TiO_2–Sb-MOF) anodes and then to study the feasibility of the MOF-PEC process in the treatment of real municipal wastewater under the visible light range (500 nm). The morphology of the mixed metal MOF electrodes was examined to study their functioning during the treatment process and to prove that their fabrication had been successful. Comparative assessment of MOF-anodes to achieve maximum treatment efficiency was observed by parametric optimization. Furthermore, various parameters of environmental concern were investigated in detail using highly efficient anode (TiO_2–Bi-MOF) in the PEC system such as micropollutants removal, disinfection, and toxicity analysis to release the treated wastewater into the open environment. A total of 77 major recalcitrant micropollutants removal efficiency was observed along with the disinfection efficiency of 23 major phyla present in the municipal wastewater. To the best of our knowledge, these types of mixed metal MOF electrodes have not been used in the literature earlier to treat municipal wastewater.

2. Materials and methods

2.1. Chemicals and municipal wastewater

Benzene-1,3,5-tricarboxylic acid ($C_6H_3(CO_2H)_3$), antimony chloride ($SbCl_3$), bismuth chloride ($BiCl_3$), praseodymium chloride ($PrCl_3$), tin chloride ($SnCl_2$), nickel chloride ($NiCl_2$), *N,N*-Dimethylformamide, DMF ($HCON(CH_3)_2$) and ferric oxide (Fe_2O_3) were purchased from Sigma Aldrich. The inflow of the municipal wastewater treatment plant in Mikkeli, Finland, was collected for PEC treatment. Samples were collected from the same inlet site at the end of every week. The main influent of the wastewater plant is municipal sewage and hospital wastewater. Detailed physicochemical characterization of the municipal wastewater was performed, and average values as presented in Table 1.

Table 1
Physicochemical characterization of municipal wastewater.

Parameters	Values
Average Temperature (°C)	10
Enterococci (CFU/100 mL)	1.27×10^6
Escherichia coli (CFU/100 mL)	9.85×10^6
pH	7.1
Electrical conductivity(mS)	90.63
Alkalinity (mmol/L)	5.48
Total solids (mg/L)	4.78×10^2
BOD (mg/L)	343
COD (mg/L)	7.32×10^2
Nitrogen (N). total (mg/L)	59.04
Ammonium nitrogen (NH_4–N) (mg/L)	46.19
Phosphorus (P). total(mg/L)	10.78
Phosphorus (P) (mg/L)	10.12
Nickel (Ni) (mg/L)	0.01
Iron (mg/L)	10.79

2.2. Preparation of MOF electrodes

A hydrothermal approach was used to prepare mixed metal MOFs of bismuth (Bi) and antimony (Sb). In this regard to prepare Bi-MOF, an equimolar concentration (0.008M) of $BiCl_3$ was added into a 2:1 ethanol: deionized water ratio and mixed with (0.004M) half molar concentration of $C_6H_3(CO_2H)_3$. Following sonicating for 30 min, the mixture was transferred to a 100 mL Teflon-lined stainless-steel autoclave and retained at 200 °C overnight. Similarly, Sb-MOF was synthesized. Furthermore, mixed metals ($PrCl_3$, $SnCl_2$, $NiCl_2$, and Fe_2O_3) were added into a 2:1 ethanol: deionized water ratio along with a half molar concentration of $C_6H_3(CO_2H)_3$. The mixture was sonicated for another 30 min, yielding a dark-colored suspension that was transferred to a 100 mL Teflon-lined stainless-steel autoclave with synthesized Bi-MOF and Sb-MOF separately and maintained at 200 °C for overnight in an oven. After cooling naturally, the suspension was filtered and washed with water and DMF several times. Furthermore, Ti seamless perforated tube (165 cm^2) purchased from global engineers, in India was used as a base material for mixed metal MOF electrode synthesis. An anodization method was used for the synthesis of the oxide layer over the surface of the Ti plate. Electrochemically a nano-layer of Bi/Sb mixed metal MOF was generated over the TiO_2 surface at 15V for 30 min and kept in the oven for 3 h at 100 °C. Lastly, the TiO_2–Bi/Sb-mixed metal MOF electrodes were obtained by washing them with acetone and deionized water successively.

2.3. Experimental setup and photo electrocatalytic experiments

The PEC experiments were performed in a circular flexi continuous mode photo-electrocatalytic reactor of working volume 1 L under the xenon lamp as a visible light source (Fig. 1). A rod shape (height = 3 cm) TiO_2–Bi/Sb (mixed-metal) MOF electrodes were used as the anode (165 cm^2), and stainless steel (165 cm^2) served as the cathode. Anodes and cathodes were fixed 1 cm apart from each other. A peristaltic pump was used to maintain the flow rate inside the PEC reactor. Potentiostat (IVIUM OctoStat5000) on mixed-mode operating conditions was used as a power system for the PEC system. To design the experiments for the optimization of PEC operational parameters, the range of selected PEC operational parameters (elapsed time, voltage, retention time (RT), and pH) was decided according to the preliminary study in terms of maximizing the % COD removal. Aliquots were sampled after a fixed interval of time for analysis. The PEC experiments were carried out in the same reactor using TiO_2–Bi-(mixed-metal) MOF and TiO_2–Sb-(mixed-metal) MOF electrodes as an anode with the same power and light source, respectively. The closed reflux method was used to calculate the COD at the end of the experiment. The % COD removal at a particular interval of time was calculated according to equation (1).

$$\%\ CODr = \left(\frac{1 - COD_t}{COD_0}\right)100 \tag{1}$$

Here, subscriptions COD_t is a COD at any time (i.e. 10, 20, 30, 40, 50, 60 …. min) and COD_0 is the initial COD of the municipal wastewater. The average current efficiency (*CE*) and energy consumption (*EEC*) are calculated as equations (2) and (3), respectively to treat per liter of the municipal wastewater in terms of COD removal.

$$Electro\ Catalytic\ Energy\ Consumption(EEC) = \left(\frac{CIt}{COD_0 - COD_t}\right)10^6 \tag{2}$$

$$Current\ efficiency(CE\ \%) = (COD_0 - COD_t) \tag{3}$$

Here, C represents average cell voltage, I represent current (A), and COD_0 and COD_t are the COD values (mg/L) at elapsed time 0 and t, respectively. V is the volume of municipal wastewater in the reactor (L) and F is the Faraday constant (96487 C/mol).

The supplementary material (Text S1) describes the analysis of municipal wastewater.

2.4. Electrodes characterization

2.4.1. Texture analysis

Brunauer–Emmett–Teller (BET) method using Tristar® II Plus instrument was employed to determine the specific surface area of the electrode material.

2.4.2. Optical properties

UV–vis diffuse reflectance spectroscopy (DRS, Cary7000, Varian, USA) was used for the investigation of the optical absorption properties of the electrodes.

2.4.3. Structural analysis

The composition of the MOF-electrodes was analyzed using an X-ray diffractometer (XRD, Empyrean series 2 PANalytical X-ray with Co-anode at 40 kW, 30 mA). The morphologies and elemental composition of MOF-electrodes were analyzed by Hitachi S-4800 field emission scanning electron microscope-Energy dispersive X-ray spectroscopy (FESEM-EDS) and the composite lattice and crystal phase was analyzed by transmission electron microscope (TEM). HORIBA Jobin Yvon Lab-RAM HR, RAMAN spectroscopy (a green laser with wavelength 514.53 nm) was used to understand the chemical and molecular interaction.

2.4.4. Electrochemical analysis

Cyclic voltammetric analysis was performed using Zahner electrochemical workstation (Potentiostat-Galvanostat) including CIMPS using

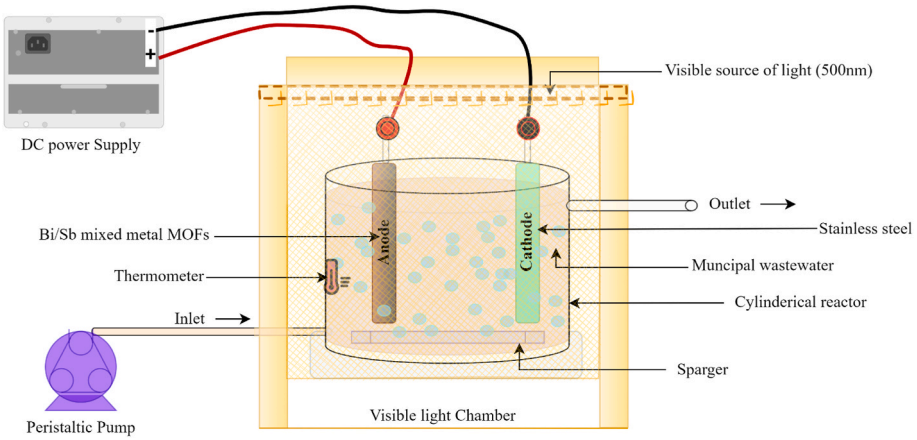

Fig. 1. Experimental setup of photo electrocatalytic system.

a typical three-electrode system. The influence of photons on the cyclic volumetry of MOF-electrodes was observed with the CIMPS system under the visible range of 500 nm. A carbon electrode was used as the reference electrode, stainless steel as a counter electrode, and MOF-electrodes as the working electrodes.

2.4.5. Stability analysis

Zahner electrochemical workstation was used to study the stability of MOF layering by the COLT (coating and laminate testing) model. AC-DC-AC surface layer stability and layer quality testing were performed.

2.5. Toxicity test

The acute toxicity evolution test was carried out using *Vibrio fischeri* (Sigma Aldrich) as the luminescent bacteria. The experiment was performed by mixing fresh bacterial culture and testing solution (1:2) and a control blank (ultrapure water). Short-term exposing the samples to 20 °C for 5 min, the bioluminescence intensity was measured by a fluorescence spectrophotometer (Thermo Scientific, USA). According to three replicates, the acute toxicity was assessed by comparing the relative inhibition (versus the blank control) of light emission.

3. Results and discussion

3.1. Characterization

3.1.1. Texture analysis

The BET analysis method was implemented to determine the specific surface area (SSA) of the scratched layer of Bi/Sb-(mixed metal) MOF from the TiO_2 base (Table 2). The measured SSA of Bi/Sb-(mixed metal) MOF was much higher than the Bi/Sb-MOF. A marked increase in SSA was found with Bi-(mixed metal) MOF. Thus, Bi-(mixed metal) MOFs with more surface area could be advantageous for the improvement of catalytic activity and mass transfer in the photo-electrocatalytic reaction.

3.1.2. Optical properties

The optical absorption properties of the Bi/Sb-(mixed metal) MOFs were explored with the UV–Vis DRS, as shown in Fig. 2(A). It reveals that the absorption intensities of Bi/Sb-(mixed metal) MOF were all higher than the Bi/Sb-MOF in the visible light region (Fig. S1). Besides, the absorption intensities of Bi-(mixed metal) MOF were higher than the Sb-(mixed metal) MOF and advantageous for the catalytic activity improvement under the range of visible light.

3.1.3. Structural analysis

The XRD spectra of synthesized TiO_2–Bi/Sb (mixed metal) MOF electrodes were examined to identify the phase composition and crystalline structure (Fig. 2(B)). The TiO_2 peaks were observed at 25.31° and 63.31° (JCPDS No. 21–1272). The separate peaks for Bi in the XRD spectrum of TiO_2–Bi (mixed metal) MOF electrode were not prominent because of its low concentration and/or the probable overlapping of peaks after MOF formation. However, very few and small Bi peaks were evident at 27.7°, 40.48°, and 46.36° (JCPDS No. 76–1730). In the case of TiO_2–Sb-(mixed metal) MOF electrodes very low-intensity Sb peaks were identified at 46.29°, 49.33°, 54.67°,55.94°,58.89°, and 59.69° (JCPDS No. 11–0689). Individual peaks of the Pr were not found in both cases, a merged peak of Pr was identified at 57.48°or 57.70° along with $Pr(OH)_3$ peak at 13.61° in TiO_2–Bi (mixed metal) MOF electrodes spectrum, in line with previous results (Gazulla et al., 2019). A merged peak of oxides of Sn, Fe, and Ni was observed at 57.48° or 57.70° (JCPDS No. 14–1445); 43.90°, 61.66° and 90.28°, as also depicted by (Kazeminezhad and Mosivand, 2014); 43.88°, 46.2°, 57.4° and 61.66° (JCPDS No. 22–1189), respectively. The presence of sharp XRD peaks depicts the crystalline structure of synthesized MOFs.

SEM-EDS was used to assess the morphology of TiO_2–Bi/Sb (mixed metal) MOF electrodes. Fig. 3(A and B) and (C, D) illustrated the formation of a uniform framework of TiO_2–Bi-(Sn-Pr-Ni-FeO) MOF and TiO_2–Sb-(Sn-Pr-Ni-FeO) MOF, respectively. The MOFs were well layered over the TiO_2 surface. The uniform coating is clearly visible in Fig. 3(A) and (C). As shown in Fig. 3(B) Bi (mixed metal) MOF was highly ordered spherical shaped randomly aligned over the TiO_2 surface. The diameter of the Bi (mixed metal) MOF (spherical shaped) was ranging from 400 to 920 nm. Nevertheless, Sb-(mixed metal) MOF shows a uniform but irregularly structured layer over the surface of TiO_2 (Fig. 3(D)). Table 3 summarizes the results of the element analysis of the fabricated electrodes conducted by EDS mapping. To determine the element distribution of heterostructures, the EDS elemental mapping method was also adopted (Figs. S2 and S3). A uniform distribution of MOF layers over the surface of TiO_2 was visible. Moreover, oxygen was found to be distributed in a circular pattern owing to the structure of MOF, and scattered oxygen may come from some oxygen-enriched species hanging on the MOF layers. The EDS elemental mapping further confirms the successful fabrication of MOF electrodes and, uniform distribution along with high crystallinity of mixed metal MOF layer over the TiO_2 surface. The diffraction peaks with high crystallinity in the XRD pattern are pertinent to the EDS mapping. The Raman spectra of Bi-(mixed metal) MOF and Sb-(mixed metal) MOF reveals the bond vibrations and structural defects induction into the MOF's lattice (Fig. S4). The peak intensity at 1359 cm^{-1} represents the bond vibration of Ni–O whereas peaks nearly 100-300 cm^{-1} confirm the bond vibration of Bi-MOF (Nguyen et al., 2020). The case of the Sb-MOF peaks ranging from 400 to 500 cm^{-1} shows vibration in the favor of defects and incorporation of heteroatoms into the ordered lattice of Sb-MOF (Shishido et al., 2000). SnO_2 bond vibrations (638 cm^{-1}) are also observed during the RAMAN analysis. Altogether XRD, EDS analysis, and RAMAN results show the high degree of incorporation of hetero-metals into the defined lattice of MOFs.

A series of successively enlarged TEM images were used to investigate the morphology of the TiO_2–Bi/Sb (mixed metal) heterostructure MOF electrodes, illustrated in Fig. 4. A layer has been scratched from the surface of the TiO_2 plate for TEM analysis. On the partially enlarged TEM images, both Bi-(mixed metal) MOF and Sb-(mixed metal) MOF had a spherical shape. Moreover, HR-TEM images (Fig. 4(C)) revealed that the Sb-(mixed metal) MOF forms a dense layer or a sheet over the TiO_2 surface.

3.1.4. Electrochemical analysis

Electrochemical analysis was performed by cyclic voltammetric comparison of Bi-(mixed metal) MOF and Sb-(mixed metal) MOF in the absence and presence of visible light (500 nm) with the potential range from −1 to +1 at the scan rate of 20 mVs^{-1} starting in an anodic direction in 1M NaOH. It was observed that the Bi-(mixed metal) MOF response represents an oxidation process with a higher potential range of +0.5V but it comes to widen under the influence of photoelectrons and holes. A similar effect was observed in the reduction process (Fig. 5(A) and C). On the other hand, Sb-(mixed metal) MOF shows an oxidation peak of nearly 0.75V by reversing the potential scan reduction peak was observed approaching -1V. However, under the influence of photoelectrons and holes, the oxidation peak was not much affected, but the reduction peak starts shifted towards −0.25V (Fig. 5(B) and D). It was concluded from the cyclic voltammetric analysis that reversibility is

Table 2
BET analysis of Bi/Sb (mixed metal) MOF and Bi/Sb MOF.

Sample	Specific surface area (m^2/g)	Pore Volume (cm^3/g)	Pore Size (nm)
Sb-(mixed metal) MOF (Scratched layer)	4.39	1.07×10^{-2}	9.75
Sb-MOF	0.02	6.5×10^{-5}	21.45
Bi-(mixed metal) MOF (Scratched layer)	2.79×10^{2}	1.8×10^{-3}	2.57
Bi-MOF	0.80	1.3×10^{-3}	6.56

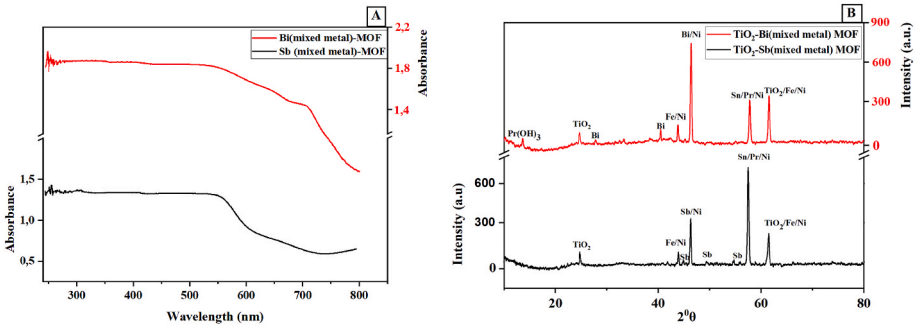

Fig. 2. **(A)** UV-DRS spectra of the Bi-(mixed metal) MOF and Sb-(mixed metal) MOF, **(B)** XRD diffractograms for the TiO_2–Bi-(mixed metal) MOF and TiO_2–Sb-(mixed metal)MOF electrodes.

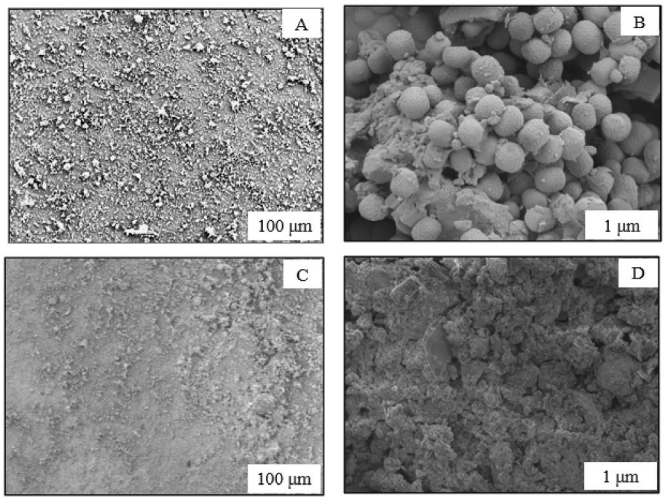

Fig. 3. SEM micrographs **(A)** Bi-(mixed metal) MOF layer electrochemically generated over the surface of TiO_2, **(B)** Magnified image of Bi-(mixed metal) MOF layer over the surface of TiO_2, **(C)** Sb-(mixed metal) MOF layer electrochemically generated over the surface of TiO_2, and **(D)** Magnified image of Sb-(mixed metal) MOF layer over the surface of TiO_2

important for the fast electron transfer kinetics and a similar trend was also observed under the influence of photons.

3.1.5. Stability analysis

The electrochemical testing of MOF layers was performed to provide electrochemical stress to the electrode by using script COLT control (AC-DC-AC). The layer quality was measured by the means of impendence, layer capacity, loss angle, and polarization at rest potential. Fig. S5 (A and B) shows the impedance curve fitting with COLT defined model for layer stability testing. It proved a good correlation between the model and observed impedance values and confirms good layer stability of MOF electrodes. Furthermore, to determine the surface stability, the impedance at rest potential was measured subsequently after 2 min of subsequent polarization phase electric stress was applied (-2V), and once again impendence was measured at new rest potential (frequency 10Hz-100KHz). In the case of the surface, stable observed data shows a good correlation with model values of impendence for both the MOF electrodes (Fig. S5 (C and D)). Therefore, from the stability analysis, it was proved that fabricated MOF electrodes were electrochemically stable for PEC experiments.

3.2. Photo-electrocatalytic degradation of municipal wastewater and optimization of process parameters

3.2.1. Effect of pH

pH is one of the key parameters that affect the efficiency of photo-electrocatalysis in wastewater treatment. The effect of wastewater pH varied from 2.5 to 10.5 for the COD removal of municipal wastewater was investigated, using TiO_2–Bi-(mixed metal) MOF and TiO_2–Sb (mixed metal) MOF electrodes. The experiments were run in triplicate and the averaged values were plotted and presented in graphs (Fig. S6). When the initial pH was 5.5, the COD removal after 180 min was 90.41% (TiO_2–Bi-(mixed metal) MOF) and 80.82% (TiO_2–Sb-(mixed metal) MOF) and when the pH was 7.5, the COD removal after 180 min was reduced to 75% and 70%, respectively.

When the initial pH was 10.5 and 3.5 only 33.50% and 59.30% of COD were removed by TiO_2–Bi-(mixed metal) MOF respectively. Similarly, in the case of TiO_2–Sb-(mixed metal) MOF electrodes, 20.15% and 51.79% COD removal were observed when the initial pH was 10.5 and 3.5, respectively. As illustrated in Fig. S6, maximum COD removal was observed in both electrodes (anode) at pH 5.5. These results show that the physical and chemical properties of metal oxides have appreciable effects on the optimum pH and photo-electrocatalysis processes during the wastewater treatment process (Liu et al., 2016; Wang et al., 2014). Comparatively, at pH 5.5, TiO_2–Bi-(mixed metal) MOF electrodes provided the highest COD removal (90.41%) than TiO_2–Sb-(mixed metal) MOF electrodes (80.82%). A slightly acidic environment of the cell accelerates the formation of •OH radicals and promotes the organic matter removal process. However, it was concluded that basic pH hinders the excitement of electrons from the semiconductor to make excited electrons and holes. However, the photoelectric-degradation efficiency was reduced due to the highly acidic pH. Acidic pH also affects the photocatalytic properties of metal oxide by cathodic displacement (Jing et al., 2010; Özcan et al., 2017).

3.2.2. Effect of voltage

Voltage is a key component in PEC processes as it controls electron

Table 3
Elemental analysis of TiO_2–Bi/Sb (mixed metal) MOF electrodes by EDS.

Electrode's	Elements	O	Ti	Fe	Sn	Sb	Pr	Ni	Bi
TiO_2–Bi (mixed metal) MOF	*Weight %*	46.51	47.86	3.06	1.04	-	0.51	0.35	0.67
	Atomic %	72.33	24.09	2.67	0.43	-	0.18	0.14	0.16
TiO_2–Sb (mixed metal) MOF	*Weight %*	63.77	26.07	3.94	3.12	2.58	0.38	0.14	–
	Atomic %	85.68	11.68	1.52	0.56	0.45	0.06	0.05	–

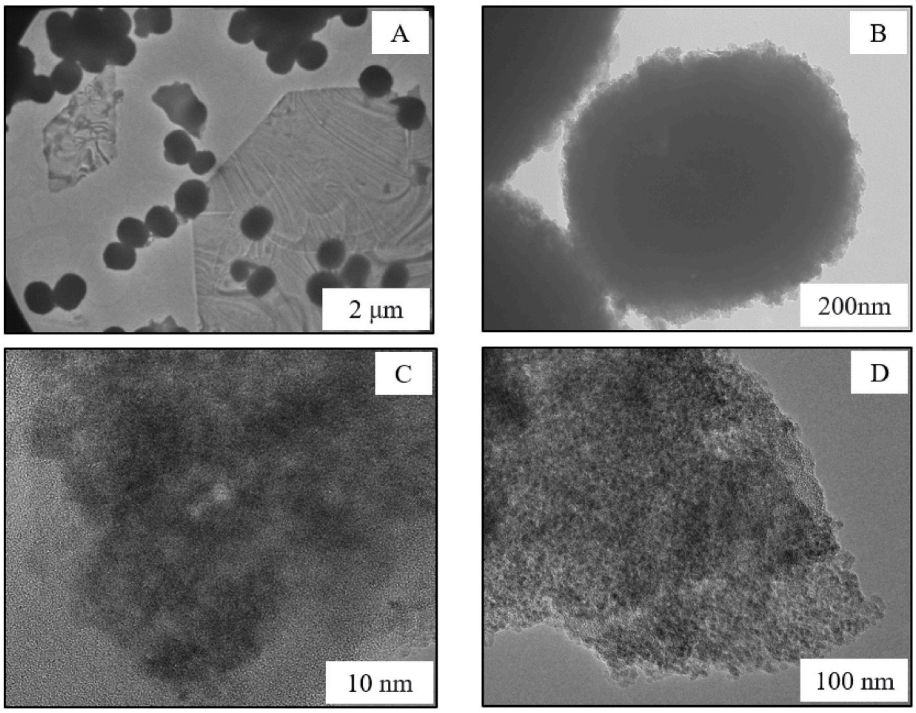

Fig. 4. TEM micrographs (**A, B**) Magnified image of Bi-(mixed metal) MOF (**C,D**) Magnified image of Sb-(mixed metal) MOF.

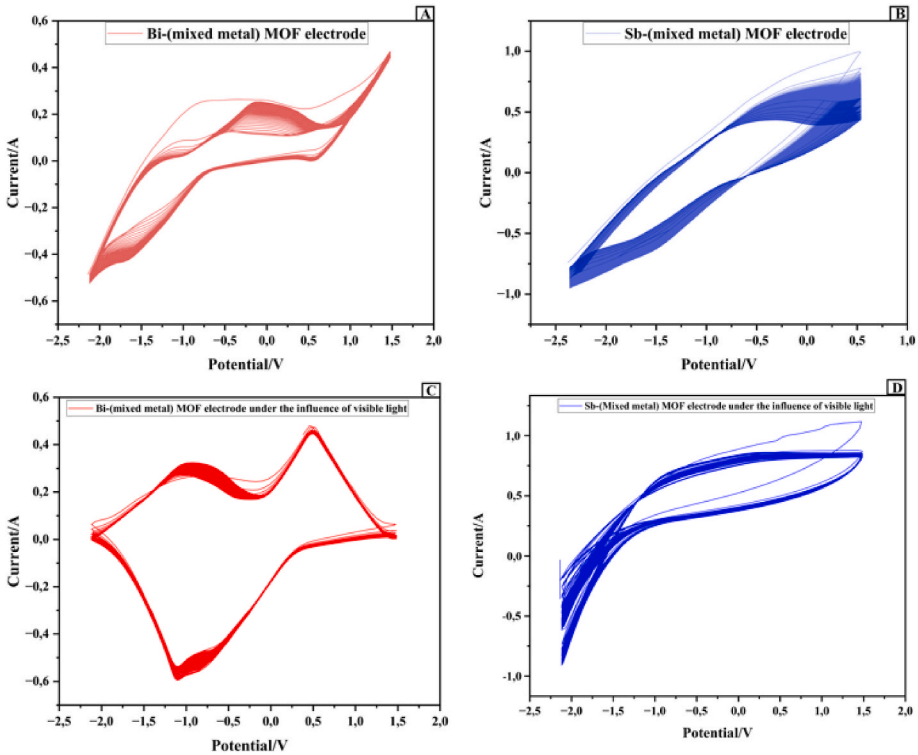

Fig. 5. Cyclic voltammetric analysis of **(A)** Bi-(mixed metal) MOF electrode **(B)**Sb-(mixed metal) MOF electrode **(C)** Bi-(mixed metal) MOF electrode under the influence of visible light (500 nm) **(D)** Sb-(mixed metal) MOF electrode under the influence of visible light (500 nm).

transfer and HO· generation (Maharana et al., 2015). Therefore, the COD removal through PEC from municipal wastewater by the synthesized bifacial (mixed metal) MOFs electrodes was investigated at varied voltage values (1–3V). There was a sudden increase in the COD removal as the voltage increased from 1 to 2V (Fig. 6(A)). Since, an increase in voltage speed up the electron transfer and accelerates the formation of active species (Zhang et al., 2020). This not only promotes the % COD removal but also led to less energy consumption (Fig. 6(B)). Nevertheless, as the voltage continued to increase, the rate of COD removal decreased instead of increasing. This could be explained by the fact that side reactions of oxygen evolution are more obvious at higher voltages (Liu et al., 2019; Dai et al., 2016). In fact, it was observed that at higher

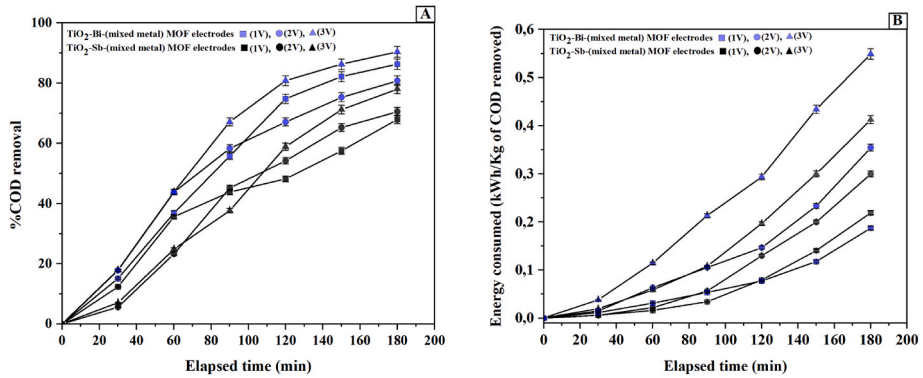

Fig. 6. (A)COD Removal by TiO_2–Bi/Sb-(mixed metal) MOF electrodes at pH 5.5 (at different cell potentials) **(B)** Energy consumed by TiO_2–Bi/Sb-(mixed metal) MOF electrodes at pH 5.5 (different cell potentials) to remove per Kg of COD from the municipal wastewater.

voltage (3V) lots of bubbles formed on the surface of the electrode. The mass transfer of organics would be alleviated by these bubbles, ultimately reducing COD removal. Moreover, reverse reaction •OH radicals in the presence of excess H_2O_2 and dimerization of •OH radicals might constrain the accessibility of •OH radicals for reaction with organics (Ouarda et al., 2020). In addition, an increase in the cell voltage promotes high energy consumption and the side reaction of oxygen evolution. When the voltage increased from 2 to 3V, electrical energy consumption was increased from 0.30 to 0.41 kWh/Kg COD removed and from 0.35 to 0.54 kWh/Kg COD removed in the case of TiO_2–Bi-(mixed metal) MOF and TiO_2–Sb-(mixed metal) MOF electrodes, respectively (Fig. 6(B)). As a result, an optimized voltage was 2V at pH 5 with minimum electrical energy consumption of 0.30 kWh/Kg COD removed with TiO_2–Bi-(mixed metal) MOF) and 0.35 kWh/Kg COD removed with TiO_2–Sb-(mixed metal) MOF electrodes. As a result, at the optimized voltage and pH (Fig. 7(A)), the current efficiency sharply increased from 3.24% to 94.11% and 3.24%–84.13% for TiO_2–Bi-(mixed metal) MOF and TiO_2–Sb-(mixed metal) MOF electrodes, respectively. This implies that during the PEC reaction at optimized voltage and pH, cell voltage fully contributes to the degradation of pollutants in municipal wastewater.

3.2.3. *Effect of retention time*

Fig. 7(B) illustrates that the COD removal increases with increasing RT. However, COD was marginally affected for all RTs more than 250 min. In the case of TiO_2–Bi-(mixed metal) MOF and TiO_2–Sb-(mixed metal) MOF electrodes this trend was observed true at the elapsed time $>$ 155 min and $>$ 165 min respectively (Figs. S7 and S8). Furthermore, at a lower RT value ($<$250 min), increasing elapsed time value always increases the COD removal. However, for all RT $>$ 250 min (TiO_2–Bi-(mixed metal) MOF), increasing elapsed time up to 150 min increases the COD removal and it was nearly unaffected for RT $>$ 250 min. Therefore, the observed steady-state elapsed time for TiO_2–Bi-(mixed metal) MOF electrodes was obtained at 155 min of elapsed time with an optimized RT is 260 min (Fig. S7). A similar trend was followed in the case of TiO_2–Sb-(mixed metal) MOF electrodes for COD removal, where increasing the RT up to 160 min sharply increases COD removal. Increasing elapsed time beyond 165 min had a marginal effect on COD removal (Fig. S8). However, for RT $>$ 250 min, when increasing elapsed time above 160 min, the COD removal remains nearly unaffected. Therefore, the observed steady-state elapsed time for TiO_2–Bi-(mixed metal) MOF electrodes was obtained at 165 min of elapsed time with optimized RT being 270 min (Fig. S8).

3.3. *Micropollutants removal at optimized operational parameters*

The LC/MS analysis was performed to investigate the micropollutants degradation efficiency along with other municipal wastewater pollutants. The major micropollutants and organic pollutants found in the Mikkeli municipal wastewater are presented in Table S1. These micropollutants are not supposed to be treated with traditional wastewater treatment plants. The initial concentration of micropollutants and the reduction in the concentration were mostly above 90% at the optimized operational parameters of the PEC treatment process, which is a very promising result. It has been observed that the PEC process was not effective for the removal of bendroflumethiazide and bezafibrate micropollutants and their concentrations in the wastewater were very low i.e. $<$0.40; 0.28, respectively. The molecular formulae of bendroflumethiazide ($C_{15}H_{14}F_3N_3O_4S_2$) and bezafibrate ($C_{19}H_{20}ClNO_4$) show the presence of fluorine and chlorine in their respective molecular structures. This proves that PEC treatment under the visible range is not effective to break the structure of this kind of

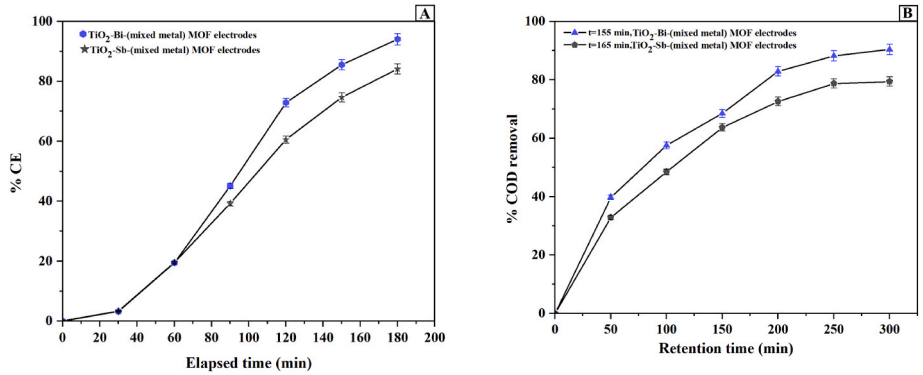

Fig. 7. (A) Current efficiency of TiO_2–Bi/Sb-(mixed metal) MOF electrodes at optimized pH (5.5) and voltage (2V) **(B)** Steady-state elapsed time for TiO_2–Bi/Sb-(mixed metal) MOF electrodes and its effect on the %COD removal with an increase of retention time.

micropollutant. This might be because of the stability of the benzene ring with the halogens, removing the electron from this type of structure needs high activation energy, which is not possible by the PEC treatment method under visible range. Few micropollutants containing halogens and benzene possibly degraded with visible light-assisted PEC treatment in the present investigation. Furthermore, a deep investigation is required to study the degradation possibility of halogen-attached benzene ring structured micropollutants by PEC treatment methods under UV and visible range of light.

3.4. Disinfection

Municipal wastewater consists of a huge amount of non-culturable microbial cells therefore PCR was performed to investigate the potential presence of these microbes in the municipal wastewater before and after PEC treatment at optimized operational conditions. The effect of PEC treatment was observed on DNA base pair count before and after treatment as shown in Table 4. The number of base pair counts for a particular phylum was reduced with the increase of elapsed time at optimized operational parameters. It is a fact that generated •OH radicals and other oxidants directly affect the DNA of the microbes, ultimately causing cell destruction (Gogniat and Dukan, 2007). The overall cell death and DNA destruction were observed based on base-pair count before and after PEC treatment using TiO_2–Bi-(mixed metal) MOF electrodes. PCR analysis exhibits that after 180 min of PEC treatment at 1.5V anode potential, genome base pairs of the bacterial phyla indicator decreased by 70%. Inclusively, the disinfection study proves that the PEC process was very effective for the disinfection of real municipal wastewater.

3.5. Toxicity test

Advanced oxidation processes as a method to degrade refractory organic compounds are effective for reducing risk to the environment by oxidizing/reducing refractory organic compounds to harmless inorganic end-products. Nevertheless, the degradation of refractory organic compounds does not always limit ecological risks. Therefore, some generated transformants during the treatment process can be more toxic or harmful as compared to their parent compounds (Da Rosa et al., 2019; Da Silva et al., 2016). In this study, toxicity during the degradation of municipal wastewater was evaluated by monitoring the bioluminescence intensity of luminescent bacteria over time. As shown in Fig. 8 the luminescence inhibition was increased from 43.6% to 58.7% in 60 min and further decreased to 35.34% within 120 min, likely because of the formation of toxic transformants. Hence, after PEC treatment of wastewater, environmental risk can be minimized by conducting a toxicity assessment.

Table 4
Disinfection study based on base pair count before and after PEC treatment.

Phylum	Base pair count (Initial)	Base pair count (After PEC treatment with Bi-(mixed metal)-MOF	Disinfection (%)
Firmicutes	12521	3724	70.26
Proteobacteria	4569	1681	63.20
Bacteroidetes	6223	3476	44.14
Actinobacteria	3032	1485	51.03
Acidobacteria	2110	1006	52.32
Aegiribacteria	1212	847	30.09
Armatimonadetes	1209	442	63.41
Synergistetes	624	416	33.29
Chloroflexi	525	387	26.30
Atribacteria	416	208	50.07
Hydrogenedentes	301	192	36.30
Calditrichaeota	260	91	65.18
Cloacimonetes	189	93	51.02
Euryarchaeota	172	117	32.03
Marinimicrobia	102	61	39.99
Thermotogae	73	58	20.43
Tenericutes	67	56	16.77
Spirochaetes	58	41	28.76
Epsilonbacteraeota	43	36	15.32
Patescibacteria	41	16	60.29
Planctomycetes	32	18	45.09
Caldiserica	29	13	54.28
WS1	26	10	61.56

4. Conclusions

In this work, we have uniformly synthesized a mixed metal MOF layer on the surface of TiO_2 (TiO_2–Bi/Sb-(mixed metal) MOF) via electrochemical deposition. Novel TiO_2–Bi-(mixed metal) and TiO_2–Sb-(mixed metal) MOF electrodes were used for performing potentiostatic PEC treatment of real municipal wastewater under visible irradiation (500 nm). We have observed for the first time that the mixed metals with the MOF significantly enhanced the visible irradiation absorbance (500 nm ~ Sunlight) and increased the PEC efficiency under ambient conditions. Moreover, the electrochemical stability of a mixed metal MOF layer on the surface of TiO_2 is quite good. The observed impedance values, confirm good layer stability of MOF electrodes. The separation of photo-generated electron/hole pairs at the MOF-TiO_2 interface was ascribed to the novel PEC property of mixed metal MOF electrodes. A comparative study between the TiO_2–Bi-(mixed metal) MOF and TiO_2–Sb-(mixed metal) MOF electrodes for the degradation of municipal wastewater proves TiO_2–Bi-(mixed metal) MOF electrode provided better separation of the photo-generated electron/hole pairs. It was observed that at the potential higher than 1.5V and up to 2V, combined electrocatalytic and photocatalytic reactions lead to the synergetic degradation of macro and micropollutants of the municipal wastewater along with the disinfection of the microbes. It is also observed for the first time that halogen-benzene structured micropollutants are hard to degrade using PEC treatment under a visible range of light. In the PEC treatment of municipal wastewater, some toxic byproducts were also generated. The current approach and synthesis of mixed metal MOF electrodes provide a route to the intense research interest in materials for PEC with enhanced photoactivity under visible irradiation for real environmental applications, lowered energy consumption, and green/clean technology. Consequently, the present work also exhibits a good potential of MOF electrodes with solar energy usage PEC system for a sustainable and low-carbon society.

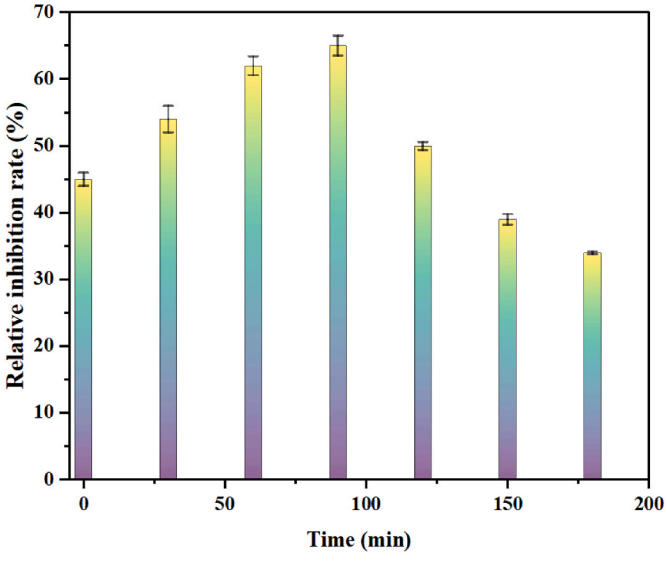

Fig. 8. Acute toxicity during the PEC treatment of municipal wastewater by the luminescence inhibition testing.

CRediT authorship contribution statement

Parminder Kaur: Investigation, Visualization, Experimental, Data curation, Writing – review & editing. **Moonis Ali Khan:** Writing – review & editing. **Yongdan Li:** Resources, Writing – review & editing. **Ahmed A.S. Al-Othman:** Conceptualization, Funding acquisition. **Zeid Abdullah Alothman:** Material testing. **Mika Sillanpää:** Conceptualization, Supervision, Funding acquisition, Validation, Resources. **Ville Kuokkanen:** Writing – review & editing, Check Industrial Feasibility. **Monzur A. Imteaz:** Writing – review & editing. **Saleh Al-Farraj:** Writing – review & editing, Funding acquisition.

Declaration of competing interest

The authors declare that they have no known competing financial interests or personal relationships that could have appeared to influence the work reported in this paper.

Data availability

Data will be made available on request.

Acknowledgments

The authors would like to express their gratitude for the financial support provided by the Distinguished Scientist Fellowship Program (DSFP) and Researchers Supporting Project Number (RSP-2023R7) King Saud University, Riyadh, Saudi Arabia.

Appendix A. Supplementary data

Supplementary data to this article can be found online at https://doi.org/10.1016/j.jclepro.2023.136165.

References

AWWA, 1999. Water Quality & Treatment: A Handbook of Community Water Supplies. McGraw-Hill, New York.
Chen, G., Chen, X., Yue, P.L., 2000. Electrocoagulation and electroflotation of restaurant wastewater. J. Environ. Eng. 126 (9), 858–863.
Cheng, H., Han, J., Nabi, I., Li, K., Wang, T., Yang, Y., Ajmal, S., Liu, Y., Zhang, L., 2019. Significantly accelerated PEC degradation of organic pollutants with the addition of sulfite and mechanism study. Appl. Catal. B Environ. 248, 441–449.
Collivignarelli, M.C., Carnevale Miino, M., Arab, H., Bestetti, M., Franz, S., 2021. Efficiency and energy demand in polishing treatment of wastewater treatment plants effluents: photoelectrocatalysis vs. Photocatalysis and photolysis. Water 13 (6), 821.
Da Rosa, A.P.P., Cavalcante, R.P., da Silva, D.A., da Silva, L.D.M., da Silva, T.F., Gozzi, F., McGlynn, E., Brady-Boyd, A., Casagrande, G.A., Wender, H., de Oliveira, S.C., 2019. H2O2-assisted photoelectrocatalytic degradation of Mitoxantrone using CuO nanostructured films: identification of by-products and toxicity. Sci. Total Environ. 651, 2845–2856.
Da Silva, S.W., Viegas, C., Ferreira, J.Z., Rodrigues, M.A.S., Bernardes, A.M., 2016. The effect of the UV photon flux on the photoelectrocatalytic degradation of endocrine-disrupting alkyl phenolic chemicals. Environ. Sci. Pollut. Control Ser. 23 (19), 19237–19245.
Dai, Q., Zhou, J., Meng, X., Feng, D., Wu, C., Chen, J., 2016. Electrochemical oxidation of cinnamic acid with Mo modified PbO2 electrode: electrode characterization, kinetics and degradation pathway. Chem. Eng. J. 289, 239–246.
Du, W., Bai, Y.L., Xu, J., Zhao, H., Zhang, L., Li, X., Zhang, J., 2018. Advanced metal-organic frameworks (MOFs) and their derived electrode materials for supercapacitors. J. Power Sources 402, 281–295.
Dubal, D.P., Jayaramulu, K., Sunil, J., Kment, Š., Gomez-Romero, P., Narayana, C., Zboril, R., Fischer, R.A., 2019. Metal–organic framework (MOF) derived electrodes with robust and fast lithium storage for Li-ion hybrid capacitors. Adv. Funct. Mater. 29 (19), 1900532.
Eckenfelder, W.W., Ford, D.L., Englande, A.J., 2009. Industrial Water Quality. McGraw-Hill Education.
Feng, J., Tian, Y., Okoth, O.K., Cheng, L., Zhang, J., 2019. Liquid phase deposition of nickel-doped ZnO film with enhanced visible light photoelectrocatalytic activity. J. Electrochem. Soc. 166 (14), H685.
Gazulla, M.F., Ventura, M.J., Andreu, C., Gilabert, J., Orduña, M., Rodrigo, M., 2019. Praseodymium oxides. Complete characterization by determining oxygen content. Microchem. J. 148, 291–298.
Gogniat, G., Dukan, S., 2007. TiO2 photocatalysis causes DNA damage via Fenton reaction-generated hydroxyl radicals during the recovery period. Appl. Environ. Microbiol. 73 (23), 7740–7743.
Han, Y., Zhou, J., Wang, L., Xing, L., Xue, Z., Jiao, Y., Pang, Y., 2021. Redox-active nanostructure electrode of Mn/Ni bimetal organic frameworks anchoring on multi-walled carbon nanotubes for advanced supercapacitor. J. Electroanal. Chem. 882, 114993.
Jing, F., Zhang, Y., Luo, S., Chu, W., Qian, W., 2010. Nano-size MZnAl (M= Cu, Co, Ni) metal oxides obtained by combining hydrothermal synthesis with urea homogeneous precipitation procedures. Appl. Clay Sci. 48 (1–2), 203–207.
Kaur, P., 2019. Treatment of Textile Effluent by Electrochemical Methods. Thapar University. Doctoral thesis. http://hdl.handle.net/10266/5472.
Kaur, P., Imteaz, M.A., Sillanpää, M., Sangal, V.K., Kushwaha, J.P., 2020. Parametric optimization and MCR-ALS kinetic modeling of electro oxidation process for the treatment of textile wastewater. Chemometr. Intell. Lab. Syst. 203, 104027.
Kazeminezhad, I., Mosivand, S., 2014. Phase transition of electrooxidized Fe3O4 to γ and α-Fe2O3 nanoparticles using sintering treatment. Acta Phys. Pol., A 125 (5), 1210–1214.
Kiama, N., Ponchio, C., 2021. Photoelectrocatalytic reactor improvement towards oil-in-water emulsion degradation. J. Environ. Manag. 279, 111568.
Kuokkanen, V., Kuokkanen, M., Hynynen, I., Kuokkanen, T., 2021. Electrocoagulation treatment of metallurgical industry wastewater–A laboratory scale batch and pilot scale continuous study. Hydrometallurgy 202, 105596.
Lecomte, S., Habauzit, D., Charlier, T.D., Pakdel, F., 2017. Emerging estrogenic pollutants in the aquatic environment and breast cancer. Genes 8 (9), 229.
Linares-Hernández, I., Barrera-Díaz, C., Roa-Morales, G., Bilyeu, B., Ureña-Núñez, F., 2009. Influence of the anodic material on electrocoagulation performance. Chem. Eng. J. 148 (1), 97–105.
Ling, L., Liu, L., Feng, Y., Zhu, J., Bian, Z., 2018. Synthesis of TiO2 mesocrystal film with enhanced photocatalytic activity. Chin. J. Catal. 39 (4), 639–645.
Liu, M., Xia, H., Lu, W., Xu, T., Zhu, Z., Chen, W., 2016. Electrocatalytic degradation of organic contaminants using carbon fiber coupled with cobalt phthalocyanine electrode. J. Appl. Electrochem. 46 (5), 583–592.
Liu, Y.J., Hu, C.Y., Lo, S.L., 2019. Direct and indirect electrochemical oxidation of amine-containing pharmaceuticals using graphite electrodes. J. Hazard Mater. 366, 592–605.
Lopez, E.C.R., Saputil, N.E.B., Loza, L.A., Camiguing, F.F.G., Mopon Jr., M., Perez, J.V.D., 2020. Iron/sulfur Co-doped titanium dioxide nanotubes: optimization of the photoelectrocatalytic degradation of phenol red under visible light. In: In Key Engineering Materials, vol. 847. Trans Tech Publications Ltd, pp. 95–101.
Maharana, D., Xu, Z., Niu, J., Rao, N.N., 2015. Electrochemical oxidation of 2, 4, 5-trichlorophenoxyacetic acid by metal-oxide-coated Ti electrodes. Chemosphere 136, 145–152.
Nguyen, V.H., Nguyen, T.D., Van Nguyen, T., 2020. Microwave-assisted solvothermal synthesis and photocatalytic activity of bismuth (III) based metal–organic framework. Top. Catal. 63 (11), 1109–1120.
Ouarda, Y., Trellu, C., Lesage, G., Rivallin, M., Drogui, P., Cretin, M., 2020. Electro-oxidation of secondary effluents from various wastewater plants for the removal of acetaminophen and dissolved organic matter. Sci. Total Environ. 738, 140352.
Özcan, A., Özcan, A.A., Demirci, Y., Şener, E., 2017. Preparation of Fe2O3 modified kaolin and application in heterogeneous electro-catalytic oxidation of enoxacin. Appl. Catal. B Environ. 200, 361–371.
Palmas, S., Mais, L., Mascia, M., Vacca, A., 2021. Trend in using TiO2 nanotubes as photoelectrodes in PEC processes for wastewater treatment. Curr. Opin. Electrochem., 100699
Panter, G.H., Thompson, R.S., Sumpter, J.P., 2000. Intermittent exposure of fish to estradiol. Environ. Sci. Technol. 34 (13), 2756–2760.
Särkkä, H., Vepsäläinen, M., Sillanpää, M., 2015. Natural organic matter (NOM) removal by electrochemical methods—a review. J. Electroanal. Chem. 755, 100–108.
Shi, H., Zhao, Y., Fan, J., Tang, Z., 2019. Construction of novel Z-scheme flower-like Bi2S3/SnIn4S8 heterojunctions with enhanced visible light photodegradation and bactericidal activity. Appl. Surf. Sci. 465, 212–222.
Shishido, T., Inoue, A., Konishi, T., Matsuura, I., Takehira, K., 2000. Oxidation of isobutane over Mo–V–Sb mixed oxide catalyst. Catal. Lett. 68 (3), 215–221.
Su, W., Chen, J., Wu, L., Wang, X., Wang, X., Fu, X., 2008. Visible light photocatalysis on praseodymium (III)-nitrate-modified TiO2 prepared by an ultrasound method. Appl. Catal. B Environ. 77 (3–4), 264–271.
Tan, H., Zhou, Y., Qiao, S.Z., Fan, H.J., 2021. Metal organic framework (MOF) in aqueous energy devices. Mater. Today 48, 270–284.
Top, S., Akgün, M., Kıpçak, E., Bilgili, M.S., 2020. Treatment of hospital wastewater by supercritical water oxidation process. Water Res. 185, 116279.
Vineyard, D., Hicks, A., Karthikeyan, K.G., Davidson, C., Barak, P., 2021. Life cycle assessment of electrodialysis for sidestream nitrogen recovery in municipal wastewater treatment. Cleaner Environ. Syst. 2, 100026.
Wang, X., Wu, P., Huang, Z., Zhu, N., Wu, J., Li, P., Dang, Z., 2014. Solar photocatalytic degradation of methylene blue by mixed metal oxide catalysts derived from ZnAlTi layered double hydroxides. Appl. Clay Sci. 95, 95–103.
Xu, Y., Jia, J., Zhong, D., Wang, Y., 2009. Degradation of dye wastewater in a thin-film photoelectrocatalytic (PEC) reactor with slant-placed TiO2/Ti anode. Chem. Eng. J. 150 (2–3), 302–307.
Zhang, Y., Xu, M., Li, H., Ge, H., Bian, Z., 2018. The enhanced photoreduction of Cr (VI) to Cr (III) using carbon dots coupled TiO2 mesocrystals. Appl. Catal. B Environ. 226, 213–219.
Zhang, Q., Zhou, Y.L., Yu, Y.B., Chen, B.Y., Hong, J.M., 2020. Exploring catalytic performance of boron-doped graphene electrode for electrochemical degradation of acetaminophen. Appl. Surf. Sci. 508, 145111.